

Lopez and Gedde<sup>29</sup> observed the development of very large spherulites (over 100  $\mu\text{m}$  in diameter) in binary blends of linear polyethylenes. At present, the study on the crystallization kinetics of this gelation crystallized UHMWPE is in progress and will be reported in a future publication.<sup>27</sup>

### Conclusions

We observed the melting and recrystallization during annealing at various temperatures near the  $T_m$  of gelation crystallized UHMWPE. The increase of SAXS long period in the present study may be due to an increase in the periodic distance of lamellar structure associated with the partial melting of certain lamellae rather than the lamellar thickening. The UHMWPE melt appears heterogeneous and anisotropic which may be a consequence of the slow diffusivity of UHMWPE chains during melting. The anisotropic melt gives rise to the small-angle scattering of X-ray and  $V_v$  light scattering. The smectic liquid crystalline structure may not be present in the UHMWPE. Large spherulites with distinct concentric fringes formed during crystallization from the melt (200  $^{\circ}\text{C}$ ), but no superstructure developed during cooling from 145  $^{\circ}\text{C}$ .

**Acknowledgment.** The support of this work by the National Science Foundation, Grants MSM-8519906 and MSW-8713531 to the University of Akron, is gratefully acknowledged. This research is also sponsored in part by the National Science Foundation under Interagency Agreement DMR-8311769 and the U.S. Department of Energy under Contract DE-AC05-84OR21400 with Martin Marietta Energy Systems, Inc.

**Registry No.** PE, 9002-88-4.

### References and Notes

- (1) Zwijnenburg, A.; Pennings, A. J. *Colloid Polym. Sci.* **1976**, *254*, 868.

- (2) Pennings, A. J.; Torfs, J. C. *Colloid Polym. Sci.* **1979**, *257*, 547.
- (3) Smith, P.; Lemstra, P. J.; Kalb, B.; Pennings, A. J. *Polym. Bull. (Berlin)* **1979**, *1*, 733.
- (4) Smith, P.; Lemstra, J. *Mater. Sci.* **1980**, *15*, 505.
- (5) Smith, P.; Lemstra, P. J.; Booi, H. C. *J. Polym. Sci., Polym. Phys. Ed.* **1981**, *19*, 877.
- (6) Smook, J.; Torfs, J. C.; van Hulten, P. F.; Pennings, A. J. *Polym. Bull. (Berlin)* **1980**, *2*, 293.
- (7) Matsuo, M.; Manley, R. St. J. *Macromolecules* **1982**, *15*, 985.
- (8) Pennings, A. J.; van der Mark, J. M.; Kiel, A. M. *Kolloid Z. Z. Polym.* **1970**, *237*, 334.
- (9) deBoer, J.; van den Berg; Pennings, A. J. *Polymer* **1984**, *25*, 513.
- (10) Matsuo, M.; Sawatari, C. *Macromolecules* **1986**, *19*, 2028.
- (11) Zachariades, A. E.; Logan, J. A. *J. Polym. Sci., Polym. Phys. Ed.* **1983**, *21*, 821.
- (12) Zachariades, A. E. *J. Appl. Polym. Sci.* **1986**, *32*, 4277.
- (13) Wunder, S. L.; Merajver, S. D. *J. Polym. Sci., Polym. Phys. Ed.* **1986**, *24*, 99.
- (14) Wunderlich, B. *Macromolecular Physics*; Academic Press: New York, 1973.
- (15) Geil, P. H. *Polymer Single Crystals*; Wiley: New York, 1963.
- (16) Schultz, J. M. *Polymer Materials Science*; Prentice-Hall: Englewood Cliffs, NJ, 1974.
- (17) Chandrasekhar, S. *Liquid Crystals*; Cambridge University Press: Cambridge, 1977.
- (18) Stein, R. S.; Rhodes, M. B. *J. Polym. Sci., Polym. Phys. Ed.* **1969**, *7*, 1539.
- (19) Kawaguchi, A.; Ichida, T.; Murakami, S.; Katayama, K. *Colloid Polym. Sci.* **1984**, *262*, 597.
- (20) Grubb, D. T.; Liu, J. H.; Caffrey, M.; Bilderback, D. H. *J. Polym. Sci., Polym. Phys. Ed.* **1984**, *22*, 367.
- (21) Grubb, D. T.; Liu, J. H. *J. Appl. Phys.* **1985**, *58*, 2822.
- (22) Fischer, E. W.; Schmidt, G. F. *Angew. Chem.* **1962**.
- (23) Fischer, E. W. *Pure Appl. Chem.* **1972**, *31*, 113.
- (24) Mandelkern, L.; Allou, A. L., Jr. *J. Polym. Sci., Polym. Lett. Ed.* **1966**, *4*, 447.
- (25) Mandelkern, L.; Sharma, R. K.; Jackson, J. F. *Macromolecules* **1969**, *2*, 644.
- (26) Chivers, R. A.; Barham, P. J.; Martinez-Salazar, J.; Keller, A. *J. Polym. Sci., Polym. Phys. Ed.* **1982**, *20*, 1717.
- (27) Kyu, T.; Cho, M. H., to be submitted for publication.
- (28) Hay, I. L.; Keller, A. *Kolloid Z. Z. Polym.* **1969**, *204*, 43.
- (29) Rego Lopez, J. M.; Gedde, U. W. *Polymer* **1988**, *29*, 1037.

## Structural Studies of Conducting Polymer Solutions and Films: Poly(3-methylthiophene)

D. Phil Murray,<sup>†</sup> Lowell D. Kispert,\* and Steve Petrovic

Chemistry Department, The University of Alabama, Tuscaloosa, Alabama 35487

Jane E. Frommer

IBM Research Division, Almaden Research Center, 650 Harry Rd., San Jose, California 95120. Received July 20, 1988;

Revised Manuscript Received October 14, 1988

**ABSTRACT:** 3-Methylthiophene has been polymerized by  $\text{AsF}_5$  in  $\text{AsF}_3$  solution to illustrate the complexity of the chemical and physical interactions which govern conducting polymer solubility and final film properties. The conducting polymer solutions and the electrically conductive films cast from them have been analyzed via solution- and solid-state NMR and EPR and SEM/EDX techniques. The  $\text{AsF}_6^-$  ion that has long been proposed as a dopant counterion has been identified at low dopant levels. Sulfur-centered radicals are observed in solution, and carbon-centered radicals are observed in the corresponding cast films. These carbon-based radicals appear to be uncorrelatable with the conductivity of the cast films. From SEM measurements, the electrical and mechanical properties of the electrically conductive poly(3-methylthiophene) films cast from solution are found to be dependent on the sample morphology.

### I. Introduction

Electrically conductive polymers are polymers with highly conjugated  $\pi$ -electron systems which although insulating in their pristine state exhibit an extremely large

increase in their electrical conductivity upon chemical or electrochemical oxidation or reduction (a process referred to as "doping"). For example, the conductivity of poly(*p*-phenylene sulfide) (PPS) increases  $10^{16}$  upon oxidative doping with  $\text{AsF}_5$ . These materials combine the properties of plastics and metals making them potentially applicable to lightweight energy storage devices and electronic circuitry devices.<sup>1,2</sup> However, most conducting polymers

<sup>†</sup> Present address: Dow Chemical, USA, M. E. Pruitt Research Center, Midland, MI 48674.

suffer from intractability and air and moisture sensitivity. For these materials to be practically applicable, they must possess good processing properties and environmental stability.<sup>1,2</sup> The conducting polymer solution of  $\text{AsF}_5$ -doped PPS in  $\text{AsF}_3$  from which high quality conducting films can be cast by solvent removal demonstrates the feasibility of solution processable conducting polymers.<sup>3</sup> Yet it still suffers from sensitivity to air and moisture which is usually encountered in normal environments. Since the initial discovery of these solutions,<sup>3</sup> the  $\text{AsF}_5$ - $\text{AsF}_3$  dopant-solvent system has been extended to the in situ polymerization and doping of polythiophene from bithiophene, poly(3-methylthiophene) from 3-methylthiophene, poly(pyrrole) from pyrrole, polyphenylene/poly(phenylene sulfide) composites from terphenyl and poly(phenylene sulfide), and polyphenylene from bi-, ter-, and sexiphenyl.<sup>2</sup> Recent articles in the literature report several conductive poly(3-alkylthiophenes) which have longer term environmental stability and are soluble in organic solvents such as nitromethane, dimethylformamide, and tetrahydrofuran; however, the precursor polymer must be prepared by another synthetic route prior to doping.<sup>4,5</sup> The in situ chemical polymerization and doping have yet to be extended to a more innocuous dopant-solvent system.

The  $\text{AsF}_5$ - $\text{AsF}_3$  dopant-solvent system is important as a model system because one can directly study the physical and chemical interactions that control the solubility in both the doping process and the film casting process. This information will be useful in extending the in situ polymerization and doping to more practical dopant-solvent systems. The in situ polymerization and doping also reduce spectroscopic interferences arising from chain end radicals that are usually present in polymers prepared by conventional methods. The macroscopic properties of these solutions and films, such as the color and stability of the solutions or the mechanical strength and conductivity of the films, and the experimental variables that control them, such as the amount of dopant added to the solution or the pressure gradient above the sample during film casting, can be correlated with the spectroscopic data to better understand the factors that influence sample properties. In addition, studies of the electronic conduction mechanism in the solution and solid state are accessible by solution- and solid-state EPR and NMR spectroscopic techniques.

We report here studies on conducting poly(3-methylthiophene) solutions made with the  $\text{AsF}_5$ - $\text{AsF}_3$  dopant-solvent system. EPR and NMR of these solutions indicate several distinct stages of varying stability in the polymerization and doping process. The method of casting the film plays a dominant role in determining the final film properties that are dependent on the sample morphology as evidenced by SEM.

## II. Experimental Section

**A. Source of Materials.** The monomer 3-methylthiophene, 3MT, obtained from Aldrich (99%+ purity), was used without further purification. The  $\text{AsF}_5$  and  $\text{AsF}_3$  were obtained from Ozark-Mahoning. The  $\text{AsF}_5$  was used without further purification. The  $\text{AsF}_3$  was vacuum distilled at 0 °C (ice water bath) immediately prior to use.

The NMR  $^2\text{H}$  lock solvents acetone- $d_6$  (99%+) and dimethyl- $d_6$  sulfoxide (DMSO- $d_6$ , 99%+) were obtained from Merck Isotopes Inc. in sealed 10-g ampules. The  $^1\text{H}$  and  $^{13}\text{C}$  primary chemical shift reference trimethylsilane, TMS, was obtained from Aldrich Chemical. Both the lock solvents and the TMS were stored over 4-Å molecular sieves in a refrigerator after opening. The  $^{19}\text{F}$  chemical shift reference trifluoroacetic acid (TFA, reagent grade) obtained from Fisher Scientific was used without further puri-

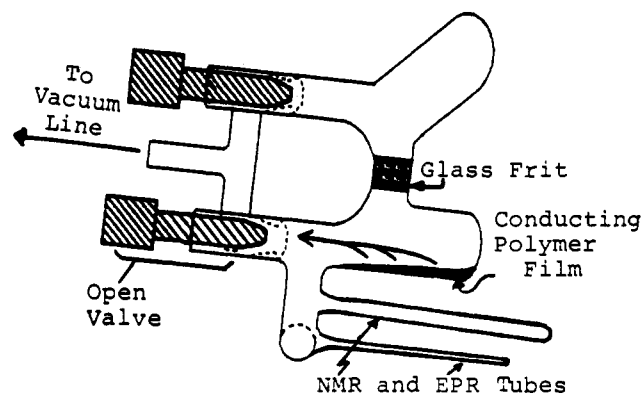


**Figure 1.** Reactor orientation during film casting. Arrow in reactor indicates pumping path.

fication. The  $^{19}\text{F}$  and  $^1\text{H}$  chemical shift reference solution, 5% TFA in acetone- $d_6$ , was made up volumetrically 10 mL at a time and stored over 4-Å molecular sieves in a refrigerator until needed.  $^{19}\text{F}$  and  $^1\text{H}$  NMR spectra of this reference solution were taken periodically to check for impurities, and fresh solutions were made up when necessary. The  $^{13}\text{C}$  chemical shift reference solution of TMS in DMSO- $d_6$  (1–2 drops of TMS in approximately 0.5 mL of DMSO- $d_6$ ) was made fresh for each sample to eliminate spectroscopic interference arising from water absorbed by the DMSO- $d_6$ .

**B. Conducting Polymer Sample Preparation.** 1. **Solution Preparation.** All  $\text{AsF}_5$ -doped poly(3-methylthiophene) solutions were prepared on a stainless vacuum line according to literature methods.<sup>2,6,7</sup> First, 0.2–0.3 ( $\pm 0.01$ ) mL of 3-methylthiophene, 3MT, was pipetted into the doping apparatus (Figure 1) under ambient laboratory conditions. Second, the reactor was connected to the vacuum line, and the 3MT degassed with at least three liquid-nitrogen ( $\text{LN}_2$ ) freeze-pump-thaw cycles. Third, 5–6 mL of  $\text{AsF}_3$  were vacuum distilled at 0 °C and then transferred into the reactor. This yielded a typical monomer concentration of 0.5–0.4 M. Fourth, the  $\text{AsF}_3$  solution of 3MT was exposed to a known volume of  $\text{AsF}_5$  dopant gas. Typically the  $\text{AsF}_5$  was held at either 0 °C or 77 K ( $\text{LN}_2$  bath) to reduce the vapor pressure of the  $\text{AsF}_5$  while the dopant was added. After the total amount of dopant gas was added, the solution was mixed then allowed to stand in the closed reactor for at least 30 min. After the solution was filtered through the glass frit of the doping apparatus (Figure 1), aliquots of the solution were transferred to glass EPR and NMR sample tubes attached to the doping apparatus (Figure 1) that were then flame sealed.<sup>7</sup> The thin-wall NMR sample tubes were immersed in an ice water bath (several degrees above  $\text{AsF}_3$ 's freezing point of  $-8.5$  °C) during flame sealing to lower the vapor pressure of  $\text{AsF}_3$ . Care was taken not to go below the freezing point in order to prevent cracking of the walls which occurred on expansion of frozen  $\text{AsF}_3$  on thawing. A detailed discussion of the stainless vacuum line, the doping levels, sample preparation conditions, and bulk observations for the P3MT samples has been given elsewhere.<sup>7</sup> Electrically conductive P3MT films were cast from the solution remaining in the doping apparatus according to the techniques described next.

2. **Film Casting.** The films were cast on the walls of the doping apparatus by one of two methods of solvent removal: (1) static or (2) dynamic vacuum pumping. The nomenclature was based on the pumping technique used during the gel to film transition. In static vacuum pumping, most of the solvent was removed by rapid dynamic vacuum pumping until the solution viscosity noticeably increased, i.e., near the onset of gelation. At this point, solvent removal was continued by repeatedly exposing the viscous solution or gel to a closed vacuum manifold which had been pumped to the range of 10–100 mTorr. The reactor was propped on its side as shown in Figure 1 once the solution had gelled. This prevented puddling in the bottom of the reactor which resulted in films that were too thick. After the film formed, the reactor was opened to a dynamic vacuum until the outgassing rate into a closed vacuum was consistently less than 2 mTorr/min.

In dynamic vacuum pumping, the reactor valve above the solution was opened slightly to a dynamically pumped vacuum

manifold. The valve was adjusted so that a film of moisture condensed (room humidity >70%) and persisted on the exterior of the cooling reactor wall which was in contact with the polymer solution. After the valve was set, it was left alone until the film was completely set. As in static vacuum pumping, the reactor was propped on its side as shown in Figure 1 to prevent puddling when the solution became very viscous. In both methods the reactors was adjusted until it was almost horizontal in order to get a more uniform film thickness. Films cast by this method were significantly harder than those cast by the static vacuum pumping method. All film samples were harvested under an Ar atmosphere in a drybox to prevent any possible degradation reactions with air and moisture.

**C. Film Compensation.** In order to examine the polymer structure in the conducting P3MT films via  $^{13}\text{C}$  cross polarization magic angle spinning (CPMAS) NMR, it was necessary to remove the inorganic arsenic fluoride counterions from the doped polymer and render the electroactive polymer nonconducting: a process referred to as compensation. The compensation procedure used for the P3MT films has previously been used with success.<sup>2,3,8</sup>

The polymer sample was first finely ground to allow thorough exposure to washes. Approximately 250 mg of the doped polymer was necessary to give the 60–100 mg of compensated polymer required for  $^{13}\text{C}$  CPMAS NMR. The sample was treated for 6–8 h in each step of the following compensation procedure. The ground polymer was first stirred in 50–100 mL of an isopropyl alcohol (IPA)–NaOH solution (pH ~10). The conducting polymer's color changed from its characteristic dark blue to a dark burgundy indicating removal of the dopant counterions. Next, the polymer was rinsed with IPA and filtered into a glass Soxhlet extraction thimble (medium porosity fritted disk). The polymer was first extracted with pure IPA then with acidified IPA (20 mL of concentrated HCl in 300 mL of IPA). The polymer was then extracted with pure IPA until the IPA was no longer acidic (pH 6.0–6.5). This was followed by an extraction with 95% ethanol to remove water-soluble impurities and then absolute ethanol to begin removing water. Finally the polymer was extracted with dry acetone (dried over 4-Å molecular sieves, pellet form) to finish the water removal. The compensated polymer was vacuum dried for approximately 6 h and stored in a desiccator. Elemental analysis of the polymers compensated in this manner indicated that all arsenic and fluorine had been removed.

**D. NMR. 1. Equipment.** All solution- and solid-state NMR spectra were acquired on a Nicolet NT-200 NMR spectrometer with a 4.7-T wide-bore Oxford magnet.  $^1\text{H}$  and  $^{19}\text{F}$  spectra of the P3MT solutions were acquired at 200 and 188 MHz, respectively, with the standard 5-mm  $^1\text{H}$  solution probe built by Nicolet which was tunable to the  $^{19}\text{F}$  resonance frequency.  $^{13}\text{C}$  solution NMR spectra were acquired at 50 MHz with either a 5-mm tuned  $^{13}\text{C}$  solution probe custom built by Doty Scientific or the standard 12-mm broad-band probe built by Nicolet.  $^{13}\text{C}$  samples for the 12-mm probe were prepared directly in a 10-mm o.d. pressure valve NMR tube from Wilmad Glass Co.<sup>7</sup>

$^{13}\text{C}$  CPMAS NMR spectra were acquired with a broad-band CPMAS probe from Nicolet. The MAS assembly was an Andrew-Beams design. The 5-mm i.d. sample rotors were constructed of Delrin and were sealed with a threaded Teflon cap.

**2. Solution-State Experiments.** The P3MT solution samples for NMR spectroscopy were flame-sealed in 4-mm o.d. NMR tubes (Wilmad Ultra Precision) as described above. These sealed tubes were run concentrically in a 5-mm o.d. NMR tube (Wilmad Royal Imperial) containing the appropriate chemical shift reference solution.  $^{19}\text{F}$  and  $^1\text{H}$  NMR spectra have been acquired for all solutions in Table I except for sample 5.

$^{19}\text{F}$  spectra were acquired with a modified one-pulse sequence which employed low-power presaturation to suppress the  $\text{AsF}_3$  resonance which dominated the standard one-pulse spectrum.<sup>6,9</sup> The  $^{19}\text{F}$  chemical shifts,  $\delta_{\text{F}}$ , were referenced to external freon,  $\text{CCl}_3\text{F}$ , using TFA as a secondary external standard:  $\delta_{\text{F}}(\text{TFA}) = -78.45$  ppm relative to  $\delta_{\text{F}}(\text{CCl}_3\text{F}) = 0$  ppm.<sup>10</sup> The  $\delta_{\text{F}}$  sign convention was positive  $\delta$  for nuclei less shielded than  $\text{CCl}_3\text{F}$  and negative  $\delta$  for nuclei more shielded than  $\text{CCl}_3\text{F}$ .

All  $^1\text{H}$  spectra were obtained by using a standard one-pulse sequence. The  $^1\text{H}$  chemical shifts were referenced to external TMS ( $\delta_{\text{H}} = 0$  ppm) using the residual acetone- $d_6$  in the acetone- $d_6$  solvent of the 5% TFA chemical shift reference solution as a

**Table I**  
**Poly(3-methylthiophene) Dopant Levels, Sample Preparation Conditions, and Bulk Observations**

sample no.	dopant level <sup>a</sup>	soln observn	film casting method; film color
1	0.1 <sup>b,f</sup>	burgundy solution, yellow-white precipitate	static vacuum; burgundy
2	0.3 <sup>b,f</sup>	dark burgundy solution, yellow precipitate	static vacuum; blue-black
3	0.5 <sup>c,f</sup>	brown solution, yellow precipitate	static vacuum; blue-black
4	1.5 <sup>e</sup>	green solution	static vacuum; black
5	2.1 <sup>e</sup>	dark blue solution	dynamic vacuum; dark blue
6	2.7 <sup>d,f</sup>	dark blue solution (see Table II)	dynamic vacuum; blue-black
7	2.7 <sup>e</sup>	dark blue solution	static vacuum; blue-black
8	4.0 <sup>e</sup>	dark blue solution	static vacuum; blue-black

<sup>a</sup> Molar ratio of reactants:  $\text{AsF}_5/3\text{-methylthiophene}$ . <sup>b</sup> A small aliquot of  $\text{AsF}_5$  of known volume and pressure added to 3-methylthiophene;  $\text{AsF}_3$  solution frozen at 77 K followed by thawing and mixing. <sup>c</sup> Procedure in (b) repeated twice. <sup>d</sup> Procedure in (b) repeated twelve times. <sup>e</sup> Bulk doped with one large aliquot of  $\text{AsF}_5$  of known volume and pressure added from the vacuum manifold. <sup>f</sup> Estimated error of approximately 25% due to pressure gauge damage.

secondary external reference. The acetone- $d_6$  gave a quintet due to the  $J^2(\text{H-D})$  coupling in the  $-\text{CD}_2\text{H}$  moiety centered at 2.04 ppm relative to internal TMS.<sup>11,12</sup> This method of referencing the  $^{19}\text{F}$  and  $^1\text{H}$  chemical shifts with the same solution reduced the time delay between  $^{19}\text{F}$  and  $^1\text{H}$  experiments which was particularly critical for the unstable solutions at lower dopant levels. The reported  $\delta_{\text{H}}$  values were not corrected for bulk magnetic susceptibility effects.<sup>7</sup>

Fully decoupled  $^{13}\text{C}$  NMR spectra of solutions 4, 7, and 8 of Table I were acquired by using a standard two-level decoupling experiment.<sup>9</sup> An additional P3MT solution with a dopant level of 2.4  $\text{AsF}_5/3\text{MT}$  was prepared directly in a 10-mm o.d. pressure valve NMR tube according to literature methods.<sup>7</sup> This tube was run concentrically in a 12-mm o.d. NMR tube containing the chemical shift reference solution. The  $\delta_{\text{C}}$ 's were referenced directly to external TMS ( $\delta_{\text{C}} = 0$  ppm). The externally referenced  $\delta_{\text{C}}$ 's observed for the 3MT in  $\text{AsF}_3$  were shifted 2.1 ppm ( $\pm 0.08$  ppm) downfield with respect to the internally referenced  $\delta_{\text{C}}$ 's reported in the literature.<sup>13</sup> A partially coupled spectrum of 3MT in  $\text{AsF}_3$  was acquired via off-resonance decoupling, ORD,<sup>9</sup> in addition to the acquisition of a fully decoupled spectrum. The residual multiplet structure arising from the residual  $^1\text{H}$ – $^{13}\text{C}$  coupling was used to assign the  $^{13}\text{C}$  peaks.

**3. Solid-State Experiments.**  $^{13}\text{C}$  cross polarization magic angle spinning (CPMAS) spectra for the compensated powders of P3MT samples 4, 5, 7, and 8 were acquired according to methods described in the literature.<sup>7,14</sup> Spinning speeds of 3.0–3.4 kHz were used in order to eliminate interferences between the spinning sidebands of the rotor material signal and the aromatic and methyl resonances of the P3MT repeat units. Dipolar dephasing spectra were acquired for peak assignment purposes.<sup>7,14</sup> The cross polarization  $^1\text{H}$   $T_1$  and variable contact time experiments were performed on the compensated sample 5 to determine the parameters necessary to acquire fully cross polarized and relaxed spectra.<sup>15</sup> The optimum cross polarization times were determined experimentally for both the aromatic and methyl carbons and found to be essentially the same (2 ms).  $^{13}\text{C}$  CPMAS NMR was attempted on two doped P3MT samples (ground and diluted 1:1 with ground glass); however, no resonance could be unambiguously assigned to the conducting polymer.<sup>7</sup>

**E. Electron Paramagnetic Resonance (EPR).** Details of EPR sample preparation and data acquisition were described

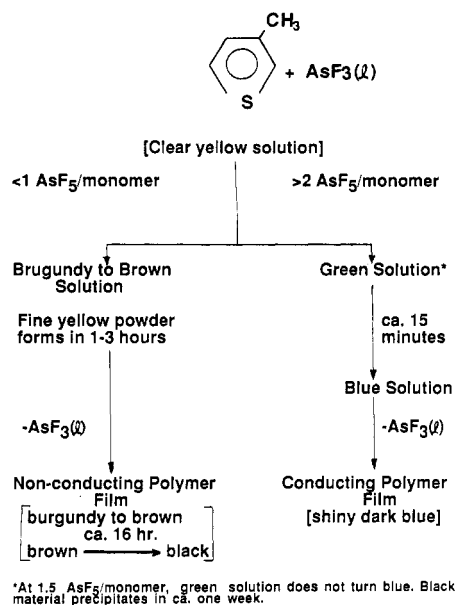


**Figure 2.** Bulk observations for the  $\text{AsF}_5$  solutions of  $\text{AsF}_5$ -doped poly(3-methylthiophene) listed in Table I.

elsewhere.<sup>6,7</sup> The unpaired spin concentration was determined according to standard methods,<sup>7,16</sup> using an EPR intensity standard, ruby (NBS SRM-2601).<sup>17</sup>

**F. Scanning Electron Microscopy and X-ray Chemical Analysis.** Scanning electron microscopy (SEM) and X-ray chemical analyses were carried out on an Etech autoscan electron microscope equipped with a Tracor Northern TN 200 energy dispersive X-ray (EDX) chemical analysis attachment.<sup>18</sup> Conducting films cast from P3MT solutions 5 and 8 were kept under argon until they were mounted on carbon pedestals with double-faced tape under ambient laboratory conditions (exposure <5 min) and then immediately transferred to a chamber which was evacuated and the films sputtered with gold-palladium alloy to prevent charging due to electron bombardment. The mounted samples were stored under vacuum in a vacuum dessicator or under argon. At least three different pieces of film were mounted on each sample pedestal such that three different film surfaces were exposed for SEM/EDX analysis. The three film samples represented three different film surfaces: (a) the one in contact with the reactor's glass wall, (b) the one exposed to the vacuum (or pressure gradient), and (c) the cross sectional cut surface perpendicular to the first two surfaces. SEM's were recorded and EDX chemical analyses were performed on the different surfaces of the film samples under the experimental conditions described in ref 7: quantitative analysis of the EDX spectra was carried out via the ZAF method<sup>18</sup> to determine the relative distribution of the elements on the film surfaces.

**G. Electrical Measurements.** Electrical conductivities ( $\sigma$ ) for irregularly shaped films and for 0.7-mm diameter pressed pellets of ground film were calculated from resistivity ( $\rho$ ) measurements according to  $\sigma = \rho^{-1}$ . The  $\rho$ 's for the samples were calculated according to eq 1<sup>19,20</sup> where  $R$  equals resistance and  $\Delta$  equals sample thickness. The resistance measurements were

$$\rho = [\pi / \ln 2] R \Delta \quad (1)$$

performed on the conducting films at room temperature under an argon atmosphere using a four-point collinear resistivity probe (Signatone)<sup>21</sup> arrangement according to methods described in the literature.<sup>7,19,20</sup> Unless otherwise noted, a minimum of three resistance measurements were made on each sample. A Hewlett-Packard 3478A digital multimeter was used to supply the current,  $i$ , and to measure the resistance,  $R$ . Details were presented in ref 7.

### III. Discussion

**A. Polymerization Mechanism.** As the molar ratio of reactants ( $\text{AsF}_5$ /3-methylthiophene) was increased, distinct color changes were observed in the solutions and in the films cast from them (Table I). The color pattern

**Table II**  
Observations and Data for Incremental Doping of Sample No. 6 in Table I

dopant aliquot no.	dopant level <sup>a</sup>	solution observations
1	0.2	burgundy solution
2	0.4	burgundy to brown opaque solution
3	0.6	brown solution
6	1.3	brown solution with green tint
7	1.5	dark green solution
12	2.7 <sup>b</sup>	dark green solution for 15 min, then dark blue solution

<sup>a</sup> Molar ratio of reactants:  $\text{AsF}_5$ /3-methylthiophene. Estimated error of approximately 25% due to pressure gauge damage. <sup>b</sup> Total dopant level after 12th aliquot; incrementally doped to this level in approximately 4 h.

is outlined in Figure 2; a burgundy to brown solution from which a nonconducting polymer was cast resulted when the molar ratio was <1 and a green to blue solution from which conductive films were cast resulted when the molar ratio was >2.

The observation of a transient green solution followed by conversion to a "stable" blue solution above 2.0  $\text{AsF}_5$ /3MT was characteristic of the P3MT solutions which yielded electrically conductive films and was used as an indicator that polymerization and doping was complete.<sup>2</sup> The term "stable" used in connection with the blue solutions denoted the absence of precipitate such as that observed for the burgundy to brown solutions (0.1–0.5  $\text{AsF}_5$ /3MT). These "stable" solutions were not indefinitely stable. Gel formation had been observed in as little as 9 days after doping in the "stable" blue solutions which were sealed in the 4-mm NMR tubes and stored in the dark. The stability of the green solution which persisted at 1.5  $\text{AsF}_5$ /3MT (sample 4, Table I) was intermediate to that of the unstable burgundy to brown solutions and the "stable" blue solutions. The transition from brown to green occurs between 1.3 and 1.5  $\text{AsF}_5$ /3MT (Table II). The occurrence of this transition at roughly 1–1.5  $\text{AsF}_5$ /3MT supported a stoichiometric (rather than catalytic) oxidative polymerization mechanism; NMR data also supported the conclusion that the  $\text{AsF}_5$ -soluble conducting polymer species formed only when an excess of  $\text{AsF}_5$  (relative to the monomer) was added.<sup>22</sup> Correlation of these visual observations with <sup>19</sup>F, <sup>1</sup>H, and <sup>13</sup>C NMR and EPR spectra of the P3MT solutions indicated the existence of different species at the various dopant levels.

**1. Solution <sup>1</sup>H and <sup>13</sup>C NMR.** The <sup>1</sup>H NMR spectra of the doped and undoped 3-methylthiophene  $\text{AsF}_5$  solutions are given in Figure 3. All three contained approximately the same concentration of 3MT in  $\text{AsF}_5$  (0.5 M). The <sup>1</sup>H NMR spectrum for 3MT in  $\text{AsF}_5$  (Figure 3a) consisted of two complex multiplets centered at 6.16 and 5.81 ppm and a singlet at 1.11 ppm with a relative peak area ratio of approximately 1:2:3, respectively. This spectrum correlated well with the spectrum of 3MT in  $\text{CCl}_4$  reported in the literature<sup>12</sup> shifted upfield due to the external referencing. At or above 1.5  $\text{AsF}_5$ /3MT, the <sup>1</sup>H NMR spectrum (Figure 3c) consisted of new peaks at 9.4, 6.7, 3.8, and 1.6 ppm. The spectrum at 0.5  $\text{AsF}_5$ /3MT (Figure 3b) exhibited resonances which corresponded to both the monomer and the new species. The low concentration of both species at 0.5  $\text{AsF}_5$ /3MT was consistent with the loss of material through precipitation.

To identify this new species, fully decoupled and off-resonance decoupled (ORD) <sup>13</sup>C spectra were acquired on a solution derived from 2.4 equiv of dopant per monomer. These spectra, shown in Figure 4, exhibited five resonances that are attributable to the thiophene moiety. [The fully

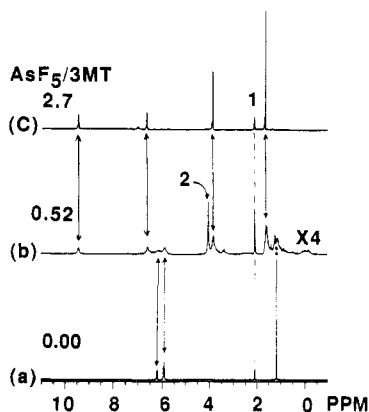


**Figure 3.** 200.1-MHz  $^1\text{H}$  NMR spectra for  $\text{AsF}_5$  solutions of  $\text{AsF}_5$ -doped poly(3-methylthiophene): (a) 3MT 0.5 M in  $\text{AsF}_5$ , (b) 0.5  $\text{AsF}_5/3\text{MT}$ , and (c) 2.7  $\text{AsF}_5/3\text{MT}$ . Peak 1 is due to residual acetone- $d_6$  in external 5% TFA in acetone- $d_6$  (all spectra normalized to this peak). Peak 2—possibly  $\text{H}_2\text{O}$  in external reference.

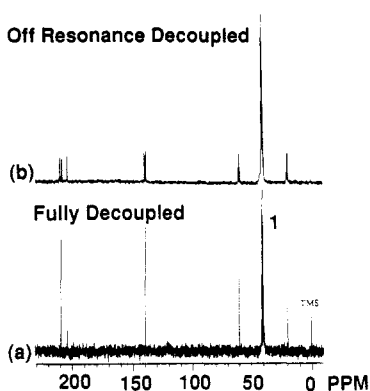
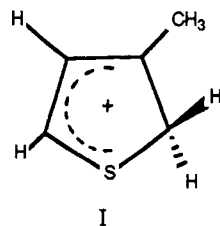


**Figure 4.** 50.3-MHz  $^{13}\text{C}$  NMR spectra for an  $\text{AsF}_5$  solution of  $\text{AsF}_5$ -doped poly(3-methylthiophene): 2.4  $\text{AsF}_5/3\text{MT}$ . TMS refers to external TMS in  $\text{DMSO}-d_6$ ; peak 1 is due to multiplet of  $\text{DMSO}-d_6$ .

decoupled spectrum in Figure 4a was identical to those recorded from solutions 4, 7, and 8 of Table I.] In the ORD spectrum in (Figure 4b), the quartet at 19 ppm and the triplet at 59 ppm corresponded to methyl ( $\text{CH}_3$ ) and methylene ( $\text{CH}_2$ ) carbons, respectively. The doublets at 139 and 208 ppm corresponded to secondary  $\text{sp}^2$  hybrid carbons, while the singlet at 203 ppm indicated a tertiary  $\text{sp}^2$  hybrid carbon. We assigned the  $^1\text{H}$  and  $^{13}\text{C}$  NMR spectra observed at and above 1.5  $\text{AsF}_5/3\text{MT}$  to the 3-methylthiophenium ion (I) based on comparison with the



$^1\text{H}$  spectra of 3-methylthiophenium in  $\text{HF}$  and  $\text{HF}\cdot\text{BF}_3$  solutions<sup>23</sup> and the  $^{13}\text{C}$  spectra of thiophenium ions in fluorosulfonic acid<sup>24</sup> at low temperatures. Since ring coupling during the polymerization process formed excess  $\text{H}^+$ 's, the formation of 3-methylthiophenium as a byproduct was quite reasonable. Noteworthy, no other NMR signals were observed which could be attributed to another solution species, such as a polymer. This was possibly due to a conducting polymer's line broadening by electron-nuclear interactions or even to lack of polymer formation

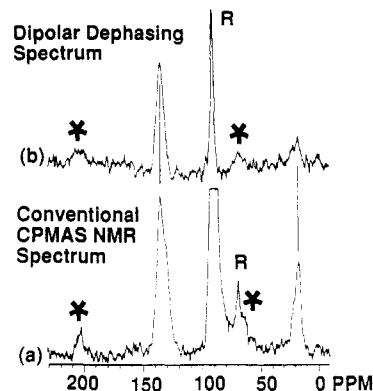
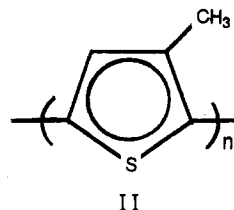


**Figure 5.** 50.3-MHz  $^{13}\text{C}$  CPMAS NMR spectra for the compensated powder of poly(3-methylthiophene) film cast from solution 5 (refer to Table I). R is the signal due to Delrin rotor material. The sample spinning sidebands are marked with an asterisk.

in solution, although the deep blue color of these solutions implied that some homologation had occurred. To resolve this question, quantitative NMR measurements must be carried out.

**2.  $^{13}\text{C}$  CPMAS NMR.**  $^{13}\text{C}$  CPMAS NMR spectra for the compensated polymer from the 2.1  $\text{AsF}_5/3\text{MT}$  solution (no. 5 of Table I) are shown in Figure 5. A similar spectrum was obtained for the compensated polymer from the 4.0  $\text{AsF}_5/3\text{MT}$  solution (no. 8 of Table I). In the conventional CPMAS spectrum (Figure 5a), the major resonances at 20 and 134 ppm and the shoulder at 130 ppm were respectively assigned to the methyl carbon, the tertiary aromatic carbons, and the secondary aromatic carbon of the 3-methylthiophene moiety. The resonances in the spectrum were easily assigned from comparison with the dipolar dephasing spectrum in Figure 5b,<sup>25</sup> the solution  $^{13}\text{C}$  NMR spectrum of 3-methylthiophene in  $\text{AsF}_3$ ,<sup>15</sup> and  $^{13}\text{C}$  CPMAS NMR spectrum for electrochemically synthesized poly(3-methylthiophene)<sup>26</sup> and from analysis of the relative peak areas.

The relative peak area analysis of the fully relaxed and fully cross-polarized CPMAS spectrum in Figure 5a gave additional qualitative information on the degree of cross-linking via the methyl groups and the degree of polymerization. The aromatic to methyl peak area ratio of 3.0–3.5 indicated that a significant amount of cross-linking via the methyl group had not occurred. Assuming the polymerization predominately proceeded via coupling at the  $\alpha$ -carbons, the degree of polymerization,  $n$ , can be related to the relative ratio ( $R$ )<sup>14</sup> of the tertiary aromatic peak area to the secondary aromatic peak area, as  $R = (3n - 2)/(n + 2)$ . For example, a monomer ( $n = 1$ ) or dimer ( $n = 2$ ) yields an  $R$  of  $1/3$  and 1, respectively. The  $R$  for the spectrum in Figure 5a was 1.4, corresponding to a trimer. Deconvolution of these peaks should result in a decrease of the shoulder intensity; therefore, the actual relative intensity ratio and thus the peak area ratio would probably be higher. These data for the compensated polymer were consistent with a structure of a minimum of three 3-methylthiophene repeat units coupled through  $\alpha$ -carbons as shown in structure II.



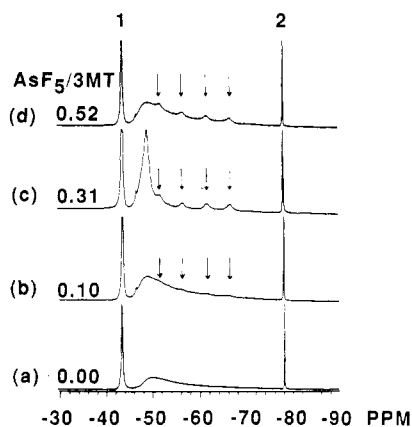


**Figure 6.** 188.2-MHz  $^{19}\text{F}$  LOSAT NMR spectra for  $\text{AsF}_5$  solutions of  $\text{AsF}_5$ -doped poly(3-methylthiophene): (a) 0.00; (b) 0.10; (c) 0.31; (d) 0.52  $\text{AsF}_5/3\text{MT}$ . Peak 1 is due to  $\text{AsF}_3$ , and peak 2 is the trifluoroacetic acid resonance (secondary external chemical shift reference); all spectra normalized to this peak.

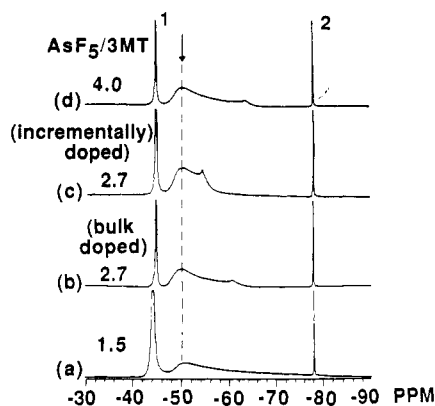


**Figure 7.** 188.2-MHz  $^{19}\text{F}$  LOSAT NMR spectra for  $\text{AsF}_5$  solutions of  $\text{AsF}_5$ -doped poly(3-methylthiophene): (a) 1.5; (b) 2.7; (c) 2.7; (d) 4.0  $\text{AsF}_5/3\text{MT}$ . Peaks 1 and 2 have been defined in Figure 6 caption.

**3. Solution  $^{19}\text{F}$  NMR.** The  $^{19}\text{F}$  low power presaturation (LOSAT) NMR spectra of the P3MT solutions below and above 1  $\text{AsF}_5/3\text{MT}$  are shown in Figures 6 and 7, respectively. These spectra illustrate the complexity of the arsenic fluoride chemistry in the polymerization, doping, and solvation processes.

The  $^{19}\text{F}$  spectrum for neat  $\text{AsF}_3$  (Figure 6a) consisted of the suppressed  $\text{AsF}_3$  resonance (peak 1) at about -44 ppm, an unidentified broad asymmetric resonance with a maximum at approximately -50 ppm, and a resonance (peak 2) for external trifluoroacetic acid, TFA, at -78.45 ppm. These three resonances were present in all  $^{19}\text{F}$  solution spectra in Figures 6 and 7. As the mole ratio of  $\text{AsF}_5/3\text{MT}$  was increased from 0.1 to 0.5 (Figure 6b-d), each spectrum exhibited a 1:1:1:1 quartet (indicated by the arrows in the figures) centered at about -59.5 ppm with an arsenic to fluorine coupling,  $J_{\text{As-F}}$ , of 934 ( $\pm 17$ ) Hz. This quartet was assigned to  $\text{AsF}_6^-$  by comparison to the spectra of  $\text{KAsF}_6$  in  $\text{AsF}_3$ ,<sup>6</sup> in TFA,<sup>10</sup> and in other solvents.<sup>27,28</sup> The  $\text{AsF}_6^-$  multiplet intensity increased with dopant concentration on going from part b to part c of Figure 6, suggesting a direct correlation between the amount of  $\text{AsF}_5$  introduced and the amount of  $\text{AsF}_6^-$  generated. The  $\text{AsF}_6^-$  resonances could no longer be detected above 1.5 equiv of dopant per monomer (Figure 7). This suggested modification of the hexafluoroarsenate anion at higher doping levels. A single peak appeared between 54 and 64 ppm in the  $^{19}\text{F}$  spectrum of 2.7 and 4.0  $\text{AsF}_5/3\text{MT}$  solutions (Figure 7b-d). The sources of both this peak and of the broad asymmetric peak at -51 ppm (that vary with the

**Table III**  
**Experimental EPR Parameters for Poly(3-methylthiophene) Solutions and Films**

sample no.	dopant level <sup>a</sup>	<i>g</i> value		line width, <sup>b</sup> G	
		soln	solid	soln	solid
4	1.5	2.0033	2.0030	7.6	2.7
5	2.1	2.0035	2.0023	7.4	3.4
6	2.7	2.0041	2.0026	7.3	4.4
7	2.7	2.0041	2.0023	7.3	4.0
8	4.0	2.0038	2.0022	8.2	3.6

<sup>a</sup> Molar ratio of reactants:  $\text{AsF}_5/3$ -methylthiophene, all samples bulk doped except sample 6. <sup>b</sup> Peak-to-peak line width measured from the first derivative spectrum.

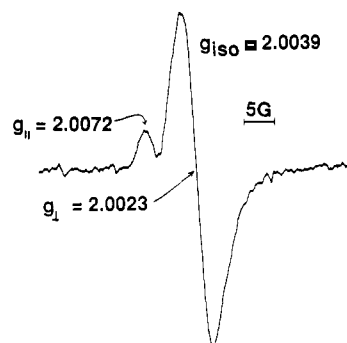


**Figure 8.** 9.5-GHz EPR spectrum for the 0.5  $\text{AsF}_5/3\text{MT}$  poly(3-methylthiophene) in  $\text{AsF}_3$  ca. 13 days after doping.

different sample preparation methods) have not been identified. The spectrum for the 1.5  $\text{AsF}_5/3\text{MT}$  solution (Figure 7a) showed no peak at all in the 50–65 ppm region of the spectrum and in fact resembled the spectrum observed for neat  $\text{AsF}_3$  (cf. Figures 6a and 7a).

**4. Solution and Solid-State EPR.** EPR spectroscopy on the same P3MT solutions as in the NMR studies was used to detect a variation in the radical species as the dopant level was changed. The burgundy to brown solutions below approximately 1  $\text{AsF}_5/3\text{MT}$  displayed quite different EPR spectra than the green and blue solutions above 1  $\text{AsF}_5/3\text{MT}$ .

In all the P3MT solutions above 1.0  $\text{AsF}_5/3\text{MT}$ , a single Lorentzian EPR signal was observed with  $g_{\text{iso}}$ 's of  $2.0038 \pm 0.0005$  (Table III). The  $g_{\text{iso}}$ 's and line widths for these P3MT solutions were comparable to those reported by Schmidt for the tetrakis(4-hydroxyphenyl)thiophene radical cation in concentrated  $\text{H}_2\text{SO}_4$  solutions.<sup>29</sup> Previously,<sup>30</sup> we reported a  $g_{\text{iso}}$  value of 2.0079 for the sulfur-based radical cation observed in conducting polymer solutions of PPS. Therefore, the solution EPR results were consistent with an oxidation of the thiophene to yield a sulfur-based radical cation.

The 0.3 and 0.5  $\text{AsF}_5/3\text{MT}$  solutions (samples 2 and 3) exhibited a very weak EPR signal at  $g_{\text{iso}} = 1.997$  when examined approximately 1 day after doping. This  $g_{\text{iso}}$  was characteristic of an inorganic radical, comparable to the  $g_{\text{iso}}$ 's reported in the literature for  $\text{AsF}_3$ ,<sup>31</sup>  $\text{AsF}_4$ ,<sup>32</sup> and  $\text{AsF}_5^-$  radicals.<sup>32,33</sup> Twelve days later sample 3 exhibited an EPR powder pattern shifted to higher  $g$  values (Figure 8). This indicated the initial presence of a solution radical species followed by the generation of a new more stable solid-state radical. A comparison of the spin counts for these two EPR spectra indicated that the initial radical species was about 100 times weaker than the solid-state species observed 13 days after doping. The powder pattern in Figure 8 was characteristic of an axially symmetric  $g$  tensor, i.e.,  $g_{xx} = g_{yy} \neq g_{zz}$  with the isotropic  $g$  value,  $g_{\text{iso}}$ , equal to 2.0039.



Table IV  
Conductivity and Radical Concentrations for the  
Conducting Poly(3-methylthiophene) Films Cast from the  
Solutions Listed in Table I

sample no.	dopant level <sup>a</sup>	sample form	$\sigma$ , <sup>b</sup> S/cm	radical concn, <sup>c</sup> monomers/ spin
1	0.1	pressed pellet	$<10^{-7}$	<i>d</i>
2	0.3	pressed pellet	$<10^{-7}$	<i>d</i>
3	0.5	pressed pellet	$<10^{-7}$	<i>d</i>
4	1.5	brittle film	0.08	456
5	2.1	hard film	19 <sup>e</sup>	466
6	2.7	hard film	28 <sup>e</sup>	180
6	2.7	pressed pellet	2.2 <sup>e</sup>	180
7	2.7	brittle film	0.16 <sup>e</sup>	794
8	4.0	brittle film	0.63 <sup>e</sup>	183
8	4.0	pressed pellet	0.45	183

<sup>a</sup> Molar ratio of reactants. All samples bulk doped except sample 6 which was incrementally doped. <sup>b</sup> Estimated error; 25–50%.

<sup>c</sup> Determined from EPR according to standard spin counting methods (refer to Experimental Section). <sup>d</sup> Below the limit of detection. <sup>e</sup> The reported  $\sigma$  is the average of measurements made on more than one pellet or piece of film.

The conducting P3MT films gave rise to an unresolved EPR powder pattern whose *g* values are given in Table III. Above 2.0 AsF<sub>5</sub>/3MT, the *g* values were typical of a delocalized carbon-based radical rather than a sulfur-based radical cation.<sup>29</sup> This carbon-based radical character in the P3MT films correlated with the XPS experimental data and theoretical calculations by Salanek and Bredas which indicated a carbon-based conductivity carrier.<sup>34</sup> It is interesting to note that the green solution at 1.5 AsF<sub>5</sub>/3MT which did not convert into the stable blue solution yet yielded electrically conductive films did not shift to a carbon-based radical in the solid state. In all the samples of Table III, line widths narrowed considerably on going from solution to solid state. This could have been due to increased electron exchange effects. At this time, no correlation can be drawn between conductivity and spin concentration for the conductive films of P3MT (Table IV).

**B. Film Morphology.** Correlation of the electrical and mechanical properties of the P3MT films with their solution and film preparation histories can provide some important clues to some of the variables that govern film properties. Although conductivity increased with increasing dopant level (Table IV), dramatic increases in conductivity were also obtained by varying the method by which the film was cast from solution (Tables I and IV). For example, P3MT solutions 5 and 7 were both doped to approximately the same dopant level by the same method: yet the films were cast from solution under the different techniques of dynamic and static vacuum, respectively (Table I). The conductivity of film cast from solution 5 under dynamic vacuum was approximately 100 times larger than that of the film cast from solution 7 under static vacuum. The film from solution 5 was very hard, requiring vigorous shaking in a stainless-steel mortar and ball pestle to grind it, whereas that from solution 7 was very brittle requiring only mild pressure from a spatula to grind it. A similar contrast in film properties resulting from different casting conditions was observed from samples 6 and 7. It was evident from these results that the film casting technique significantly affected not only the electrical but also the mechanical properties of the films cast from solution. In fact, moderate changes in the dopant level appeared to affect the film conductivities less than the film casting technique (Table IV).

The variation in the electrical and mechanical properties

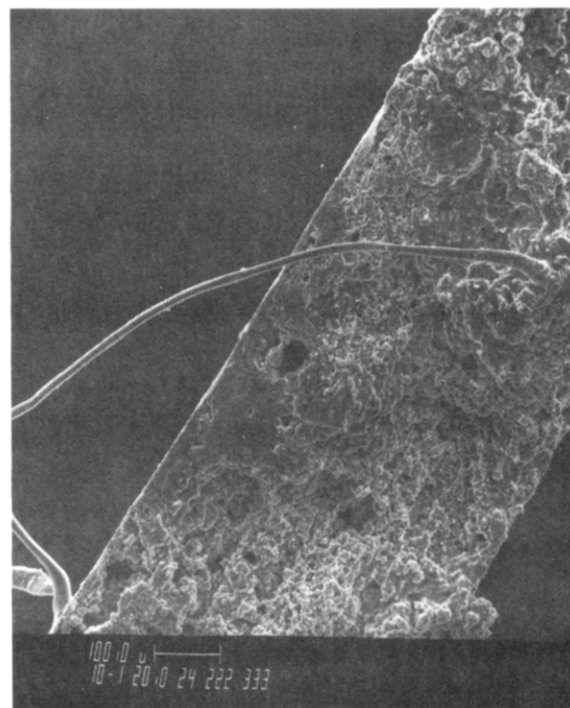
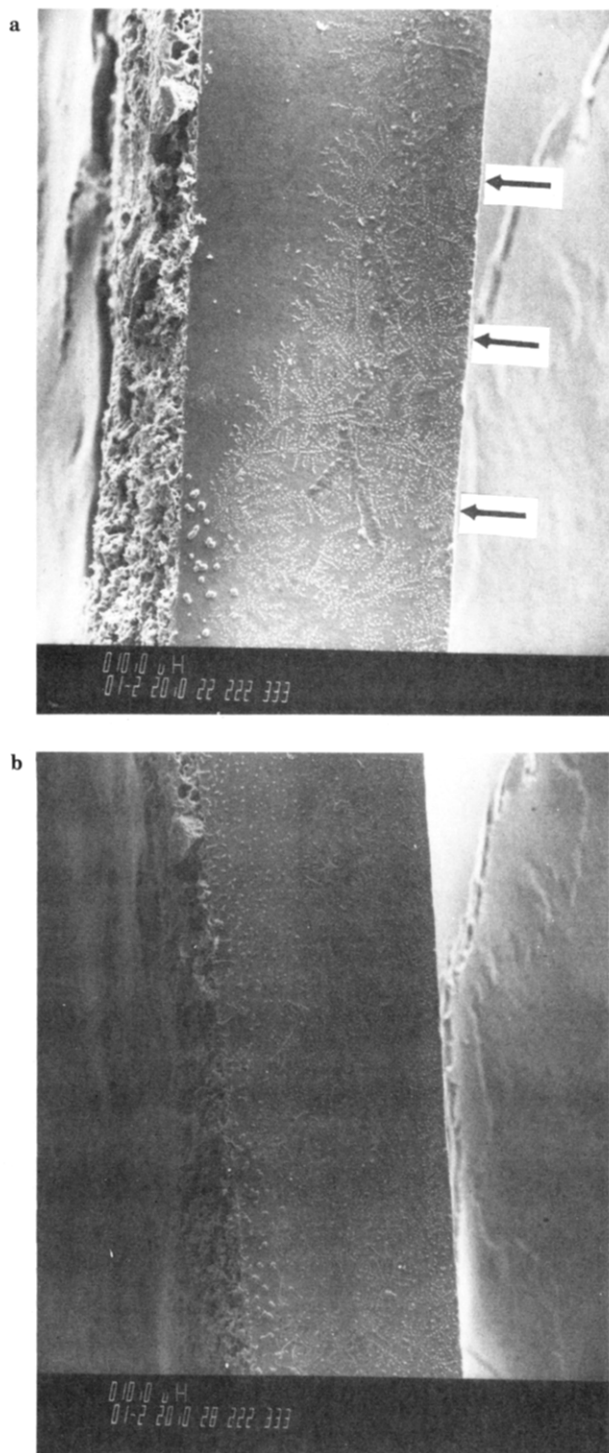


Figure 9. SEM of electrically conductive poly(3-methylthiophene) film cast from solution 8 (see Table I) using a static vacuum pumping technique resulting in a porous structure: cross sectional view. Magnification = 50.

of the P3MT films cast by the different techniques can be attributed to microscopic morphological dissimilarities as evidenced in SEM micrographs for cross sections of cast films (Figures 9 and 10a). The contrast between the compact morphology of the hard film cast from solution 5 and the porous morphology of the brittle film from solution 8 could account for the observed differences in conductivity and hardness. Lower interparticle resistance in a compact morphology leads to the observed higher conductivity of these hard films.<sup>1</sup>

The different morphologies might be attributed to the pressure gradient during the gel to film transition. In the static vacuum pumping technique, the large pressure gradient repeatedly applied in a cyclic manner tended to induce rapid outgassing of AsF<sub>3</sub>, forming voids in the semisolid matrix and resulting in a porous superstructure. On the other hand, the dynamic vacuum throttle pumping technique applied a small continuous pressure gradient to the semisolid during the gel to film transition, possibly simulating a more "diffusion-controlled" removal of the AsF<sub>3</sub>, slowly collapsing the gel to a more compact film.

Fibrillar and globular structures appeared on the cross-sectional surface of the sputter coated compact film sample 5 (Figure 10a) after storage for 2 weeks in a vacuum desiccator (Figure 10b). These new fibrillar structures, shown at higher magnification in Figure 11a (marked by a and b), appeared to be cross sections of layer structures jutting out of the smooth dark surface. They had As/S ratios by EDX chemical analysis of 4.6 and 6.4 for a and b, respectively, and 0.9 for the surrounding dark area. A value of 0.8 for the As/S ratio was found initially (Figure 10a) for the dark areas, similar to those determined by elemental analysis for the same sample (0.7–0.8).<sup>35</sup> Both areas showed the presence of Si, presumably arising from HF etching of the glass reactor. The white globular structures shown at higher magnification in Figure 11b were electron beam sensitive:<sup>18</sup> compare spot a which was irradiated to spot b which was not. On the basis of the SEM/EDX analysis, the fibrillar structures could be due



**Figure 10.** SEM's of electrically conductive poly(3-methylthiophene) film cast from solution 5 (see Table I) using a dynamic vacuum throttle pumping technique resulting in a compact film: cross sectional view. (a) SEM taken immediately after removal from argon atmosphere, magnification = 50. (b) SEM of the same region taken ca. 2 weeks later, magnification = 50.

to slow diffusion of residual solvent ( $\text{AsF}_5$ ) or dopant ( $\text{AsF}_5$ ) out of the polymer matrix to form superficial, inorganic complexes giving rise to the chemical heterogeneity of the two areas.

#### IV. Conclusions

The spectroscopic results and the macroscopic changes in the  $\text{AsF}_5$ -doped P3MT solutions provide insight into the complex chemistry of the polymerization and doping and casting processes. The solutions displayed distinct stages of varying stability with which different molecular species

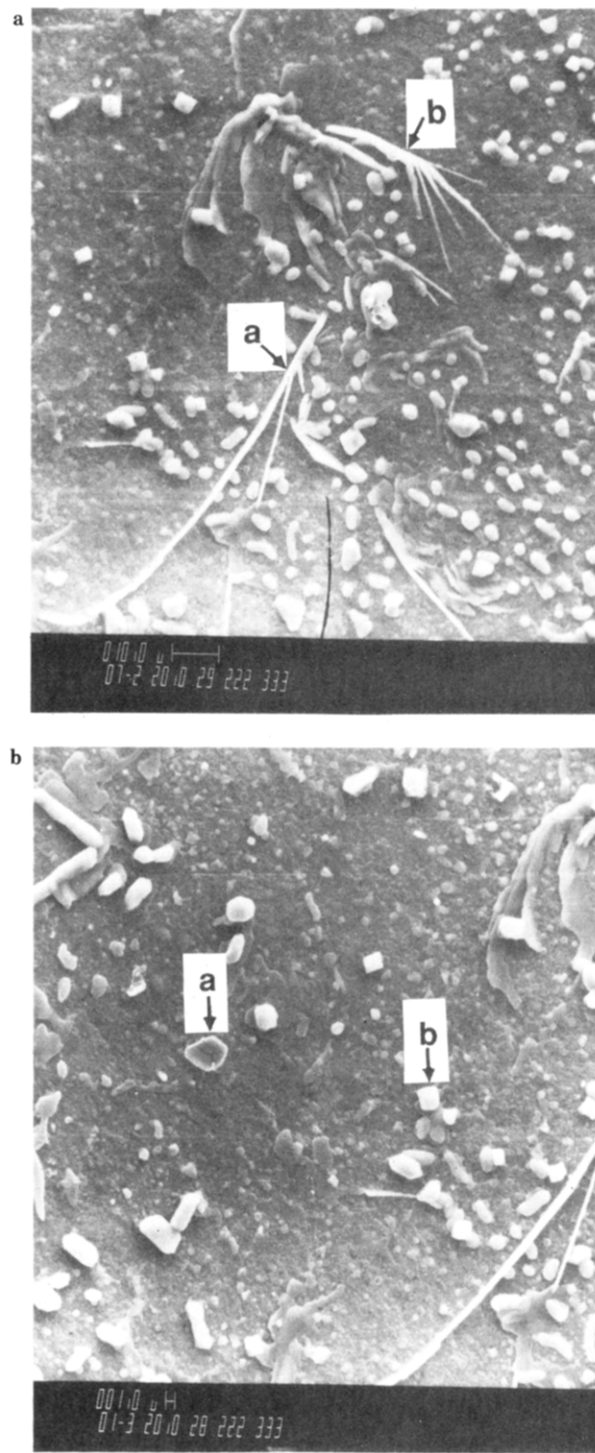


**Figure 11.** Higher magnification SEM of the sample 5 film cross section shown in Figure 10b. (a) "Fibrillar" structures, positions a and b indicate location of EDX analyses, magnification = 350. (b) Globular structures, a indicates an electron beam damaged structure and b indicates an undamaged structure, magnification = 500.

were associated. A transition from an unstable solution which yielded nonconducting film to a stable solution which yielded conducting film occurred at about 1 equiv of  $\text{AsF}_5$  dopant per equivalent of 3MT. The  $^{13}\text{C}$  CP/MAS NMR from compensated films indicated that a poly(3-methylthiophene) polymer was generated; the polymerization probably involved a stoichiometric oxidative ring coupling.

The carbon-based radical in the solid state appeared to be an uncorrelatable contributor to the electronic conduction mechanism. This left open the possibility that the



electronic conductivity mechanism was diamagnetic in nature.

The dependence of conductivity and hardness on morphology clearly demonstrated the importance of film casting parameters in controlling film properties. The SEM results for the AsF<sub>5</sub>-doped poly(3-methylthiophene) films helped explain that the 2 orders of magnitude increase in conductivity on changing the rate of solvent removal could be attributed to a decrease in interparticle resistance or more simply to an increase in bulk connectivity.

**Acknowledgment.** This work was supported by the Division of Chemical Sciences, Office of Basic Energy Sciences, Office of Energy Research of the U. S. Department of Energy under Grant No. DE-FG05-886ER13456. We thank Dr. Jim Dechter of ARCO for many helpful discussions regarding NMR techniques and Deb Clayton at the University of Alabama Biology Department for the invaluable assistance in obtaining the SEM/EDX data. Allied Signal Corporate Technology is acknowledged for chemicals and speciality materials. We would also like to thank Drs. M. Cava, M. V. Lakshmikanthan, R. Elsenbaumer, M. Maxfield, L. Shacklette, N. Forbes, and B. Hammond for helpful discussions. Special thank go to M. Watson, H. Moore, and B. James for fabrication of various components and E. Jackson for typing the manuscript.

**Registry No.** P3MT, 84928-92-7; AsF<sub>5</sub>, 7784-36-3.

## References and Notes

- Frommer, J. E.; Chance, R. R. In *Encyclopedia of Polymer Science and Engineering*, 2nd ed.; Grayson, M., Kroschwitz, J., Eds.; Wiley: New York, 1986; Vol. 5, pp 462-507. Thorough review covering conducting polymer research and development over the past decade.
- Frommer, J. E. *Acc. Chem. Res.* **1986**, *19*, 2-9 (review).
- Frommer, J. E.; Elsenbaumer, R. L.; Chance, R. R. *Org. Coat. Appl. Polym. Sci. Proc.* **1983**, *48*, 552.
- Elsenbaumer, R. L.; Jen, K. Y.; Oboodi, R. *Synth. Met.* **1986**, *15*, 169-74.
- Hotta, S.; Rughooputh, S. D. D. V.; Heeger, A. J.; Wudl, F. *Macromolecules* **1987**, *20*, 212-15.
- Frommer, J. E.; Murray, D. P.; Kispert, L. D. *Synth. Met.* **1986**, *15*, 259-63.
- Murray, D. P. Ph. D. Dissertation, University of Alabama, Tuscaloosa, AL; 1987; *Diss. Abstr. Int.*, *B* **1988**, *48*(9), 2659. Copies of the dissertation, entitled "Structural Studies of Conducting Polymer Solutions and Films: Poly(3-methylthiophene), Poly(*p*-phenylene Sulfoxide) and Related Polymers", can be purchased on microfilm or paper from Dissertation Abstracts International by calling 1-800-521-3042, order no. DA8727148.
- Frommer, J. E., technique developed at Allied-Signal Corp.
- Martin, M. L.; Martin, G. J.; Delpuech, J.-J. *Practical NMR Spectroscopy*; Heyden & Son: Philadelphia, PA, 1980; pp 177-86.
- Emsley, J. W.; Phillips, L. *Prog. Nucl. Magn. Reson.* **1971**, *7*, 17.
- This  $\delta_H$  is reported in a technical bulletin from Merck and Co. (4545 Oleatha Ave., St. Louis, MO 632116). It was measured for a solution of 5% TMS in acetone-*d*<sub>6</sub> (v/v) on a Varian HA-100 NMR spectrometer.
- The Sadtler Handbook of <sup>1</sup>H NMR Spectra*; Simons, W. W., Ed.; Sadtler: Philadelphia, PA, 1978.
- Breitmaier, E.; Haas, G.; Voelter, W. *Atlas of <sup>13</sup>C NMR Data*; Heyden & Son: Philadelphia, PA, 1979; Vol. 2, ref no. 2206.
- Murray, D. P.; Dechter, J. J.; Kispert, L. D. *J. Polym. Sci., Polym. Lett. Ed.* **1984**, *22*, 519-22.
- Murray, D. P.; Kispert, L. D.; Frommer, J. E., unpublished results.
- Randolph, M. L. In *Biological Applications of Electron Spin Resonance*; Swartz, H. M., Bolton, J. R., Borg, D. C., Eds.; Wiley-Interscience: New York, 1972; Chapter 3.
- Electron Paramagnetic Resonance Intensity Standard: SRM-2601; Description and Use*; National Bureau of Standards, Special Publication 260-59.
- Goldstein, J. I.; Newbury, D. E.; Echlin, P.; Joy, D. C.; Fiori, C.; Lifshin, E. *Scanning Electron Microscopy and X-Ray Microanalysis*; Plenum: New York, 1981.
- Wieder, H. H. *Laboratory Notes on Electrical and Galvanomagnetic Measurements*; Elsevier Scientific Publishers: New York, 1979; Chapter 1.  $\rho$  is derived for an essentially infinite conducting sheet of infinitesimal thickness; i.e.,  $\Delta \ll s$  where  $\Delta$  is the sample thickness,  $s$  is the probe spacing, and  $R$  is the resistance. Equation 1 is adequate for  $\Delta/s < 0.4$ ; however, the  $\rho$ 's for samples with  $\Delta/s$  between 0.4 and 2.0 can be corrected or errors estimated from correction factors derived by Smits.<sup>20</sup>
- Smits, F. M. *Bell Syst. Tech. J.* **1958**, *37*, 711-8.
- Signatone, 3687 Enochs St., Santa Clara, CA 95051; telephone: (408)732-3280.
- Rajappa, S. In *Comprehensive Heterocyclic Chemistry*; Katritzky, A. R., Rees, C. W., Eds.; Pergamon Press: New York, 1984; Vol. 4, Chapter 3.14, p 779 ff.
- Hogeveen, H. *Rec. Trav. Chim. Pays-Bas* **1966**, *85*, 1072-6.
- Hogeveen, H.; Kellogg, R. M.; Kuindersma, K. A. *Tetrahedron Lett.* **1973**, (40), 3929-32.
- Aleman, L. B.; Grant, D. M.; Alger, T. D.; Pugmire, R. J. *J. Am. Chem. Soc.* **1983**, *105*, 6697-704.
- Osterholm, J.-E.; Sunila, P.; Hjertberg, T. *Synth. Met.* **1987**, *18*, 169-76.
- Baliman, G.; Pregosin, P. S. *J. Magn. Reson.* **1977**, *26*, 283-9 and references cited therein.
- Mooney, E. F. *An Introduction to <sup>19</sup>F NMR Spectroscopy*; Heyden & Son: New York, 1970; Chapter 6.
- Schmidt, U. *Angew. Chem., Int. Ed. Engl.* **1964**, *3*, 602-8.
- Murray, D. P.; Kispert, L. D.; Frommer, J. E. *J. Chem. Phys.* **1985**, *83*, 3681-84.
- Subramanian, S.; Rogers, M. T. *J. Chem. Phys.* **1972**, *57*, 4582-9.
- Boate, A. R.; Colussi, A. J.; Morton, J. R.; Preston, K. F. *Chem. Phys. Lett.* **1976**, *37*, 135-7.
- Morton, J. R.; Preston, K. F.; Stach, S. J. *J. Magn. Reson.* **1980**, *37*, 321-30.
- Salaneck, W. R.; Wu, C. R.; Inganas, O.; Osterholm, J. E.; Bredas, J. L. *Abstracts of Papers*, 192nd National Meeting of American Chemical Society, Anaheim, CA; American Chemical Society: Washington, DC 1986; INOR 375.
- Murray, D. P.; Leone, E.; Kispert, L. D.; Frommer, J. E. *J. Chem. Phys.*, manuscript in preparation.